RAPID COMMUNICATIONS

PHYSICAL REVIEW E VOLUME 50, NUMBER 1 JULY 1994

Advanced chaos forecasting

R. Doerner,* B. Hübinger, and W. Martienssen

Physikalisches Institut der J. W. Goethe-Universität, Robert-Mayer-Strasse 2-4, D-60325 Frankfurt am Main, Germany

(Received 7 March 1994)

The exponential separation of initially adjacent trajectories restricts the predictability of deterministic chaotic motions. The predictability depends on the initial state from where the trajectory starts that shall be forecasted. By calculating the predictability simultaneously with the forecast, we are able to reject forecasts with low reliability immediately, thereby decreasing drastically the average forecast error. We test this scheme experimentally on Chua's circuit [Komuro, Tokunaga, Matsumoto, Chua, and Hotta, Int. J. Bifurc. Chaos **1**, 139 (1991)], basing all calculations only on a time series of a single scalar variable.

PACS number(s): 05.45.+b

The motion of a nonlinear dynamical system in the chaotic phase is not predictable for long time intervals because forecasting errors in the mean grow exponentially with the length of the forecasting time. On the average the rate of this growth is given by the sum of the positive Lyapunov exponents of the system (more precisely, by its Sinai-Kolmogorov entropy) [1], quantifying globally the separation of initially adjacent trajectories. For a single forecast, however, a local rather than a global growth rate determines the probability for a successful forecast. This rate can be described by effective Lyapunov exponents [2–4] as a quantity showing large variations, depending on the initial conditions of the forecast.

In a recent paper [5] we have demonstrated that the effective Lyapunov exponents are smooth functions of the state space coordinate $\mathbf{X}(0)$, representing the starting point of a trajectory segment. They also, of course, depend on the forecasting time interval T. We have displayed these functions in *predictability portraits*, which we produce by coloring the points in the state space according to the value of local predictability. To this end the effective Lyapunov exponents have to be calculated. They can be calculated from the equations of motion of the system, but they can also be computed from the time series of a single variable. In a second paper [6] we have argued how the geometric shape of these portraits is related to the set of unstable periodic orbits embedded in the attractor [7–9].

In this paper we demonstrate that the *a priori* knowledge of predictability can be used to improve forecasting for chaotic motions. We test our method in an experimental situation, in which all information necessary to calculate forecasts as well as necessary to calculate predictabilities is extracted from a scalar time series of a single chaotic variable. As a test system we utilize an experimental realization of Chua's circuit. We demonstrate in our example that a drastic reduction of large forecasting errors is yielded by making use of system knowledge from the effective Lyapunov exponents.

In [5] we have defined the term predictability $p(\mathbf{X}(0),T,\epsilon_0,\epsilon_T)$ as the probability of a successful forecast. It depends on the state $\mathbf{X}(0)$ of the system where the forecast is made, on the forecasting time interval T, on the uncertainty of measurement ϵ_0, and on the admitted error ϵ_T. Forecasts of the state of the system at the end of the time interval T that meet, up to an error lower than or equal to ϵ_T, the state through which the system at the same time actually moves, are called successful. We have shown that the so-defined predictability is related to the largest effective Lyapunov exponent $\lambda_{\text{eff}}^{(1)}(\mathbf{X}(0),T)$ via

$$p(\mathbf{X}(0),T,\epsilon_0,\epsilon_T)\approx \text{const}\times\frac{\epsilon_T}{\epsilon_0}\exp[-\lambda_{\text{eff}}^{(1)}(\mathbf{X}(0),T)T]$$

in the linear approximation. A Poincaré section or a projection of the state space, that is colored according to $\lambda_{\text{eff}}^{(1)}(\mathbf{X}(0),T)$, constitutes the above mentioned predictability portrait.

For the calculation of effective Lyapunov exponents from a scalar time series $\{x(i),\ i=0,1,2,\ldots,N\}$ one has to make use of the embedding technique, proposed by Takens [10]. As soon as the state space is reconstructed, forecasts of the further evolution of the system based on a measurement of its actual state can be performed by the technique of local prediction. To this end we follow the work of Eckmann *et al.* [11] and of Brown, Bryant, and Abarbanel [12]. First one has to search for nearest neighbors of the measured state on the reconstructed attractor. Then one has to determine the successors to which the neighbors have developed during the time interval T. To these points a local predictor has to be fitted, e.g., polynomials of degree 1 or higher. The forecast then is obtained as that point in state space to which the measured state is mapped by the local predictor. A suitable fit procedure is described in detail in [4].

One can calculate, however, not only forecasts but also predictabilities at the measured initial states in the reconstructed state space. Let $\mathbf{f}^T$ be the local predictor and $\mathbf{z}(0)$ the distance between two adjacent trajectories in the domain of $\mathbf{f}^T$. Within the forecasting time interval T the jth component of $\mathbf{z}(0)$ becomes

$$z_j(T)=\sum_k \mathbf{Df}^T_{jk}z_k(0)+\sum_{k,l}\frac{\partial^2\mathbf{f}^T}{2\partial y_k\partial y_l}z_k(0)z_l(0)+\cdots.$$

The largest effective Lyapunov exponent can be calculated from the linearized predictor $\mathbf{Df}^T$. Let

*Electronic address: doerner@physik.uni-frankfurt.de

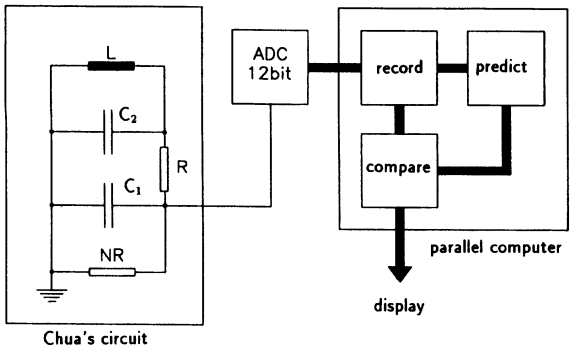

FIG. 1. Block wiring diagram of the experimental setup. ADC denotes analog-to-digital converter.

$$\mathbf{Df}^T = \mathbf{QP}$$

be the polar decomposition of the linearized flow, then the following relation holds [2]:

$$\exp(\lambda_{\text{eff}}^{(i)} T) = \rho^{(i)}(\mathbf{P}),$$

with $\rho^{(i)}$ denoting the ith eigenvalue.

With the knowledge of $\lambda_{\text{eff}}^{(1)}$ one can reduce the average forecast error, if it is possible to elude forecasting when the system is located in a state of bad predictability. Forecasts, for example, might be accepted only if $\lambda_{\text{eff}}^{(1)}$ is below a fixed value; all others are rejected.

The experimental system we use to test this method is an electronic realization of Chua's circuit [16] proposed by Kennedy [13]. Chua's circuit is a well-known nonlinear autonomous system [14–16] that exhibits various types of attractors—including two strange ones—depending on the choice of the system parameters.

Figure 1 shows a block wiring diagram of our experimental setup. The circuit consists of an inductance L, two capacitors C_1, C_2, the resistor R, and the nonlinear resistor NR. This device is built by two operational amplifiers; it possesses a piecewise linear characteristic with negative slope. For further details of the circuit design see [13]. We drive the system at parameters leading to the "double scroll attractor" [16], plotted in Fig. 2. As chaotic time series $\{x(i),\ i=0,1,2,\ldots,N\}$ the voltage at the capacitor C_1 is sampled by an analog-to-digital converter with 12 bit resolution. Then the signal is fed into a parallel computer network. In our experiment two consecutive time series (each 2.5×10^5 points) are sampled. The first is used to reconstruct the attractor; the second is used as a set of initial conditions for the calculation of forecasts as well as to calculate the forecasting errors in order to test the method. In general, the dimension of the embedding space should be $2D+1$, where D means the Hausdorff dimension of the attractor [10]. Using the Grassberger-Procaccia analysis [17] we find that a three-dimensional space embeds the dynamics of the system sufficiently at our parameters, analogously to the result for the Lorenz equations in [18]. The state vectors are represented by $\mathbf{X}(i)=(x(i),x(i-1),x(i-2))$. As the delay time between successive points we choose a quarter of the average time the state of the system needs for one circulation on a scroll. For the sake of simplicity we choose the delay time for reconstruction and the time between two measurements to be the same, leading to the sampling frequency 10 kHz.

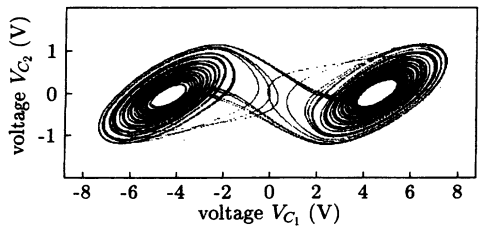

FIG. 2. The double-scroll attractor of Chua's circuit projected onto the (V_{C1}, V_{C2}) plane.

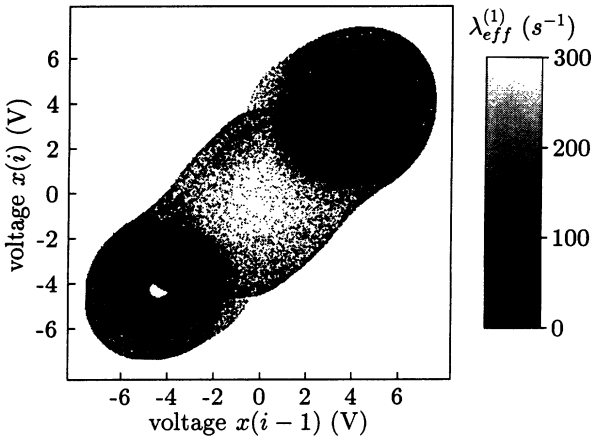

FIG. 3. A predictability portrait of the reconstructed double-scroll attractor. The forecasting interval is $T=1$ ms. Note the spiral structure on each of the two scrolls. Between the scrolls the brightness is caused by the low density of points, not by a large effective Lyapunov exponent.

In Fig. 3 we present a predictability portrait of the double-scroll attractor in the reconstructed state space. The forecasting interval here lasts 10 delay units (=1 ms). The gray level of each point encodes the corresponding largest effective Lyapunov exponent. Similar to the results presented in [5,6] the portrait exhibits smooth, well-defined zones of decreased predictability, dotted brightly upon each of the scrolls. This result can be understood qualitatively as follows: In the dark zones the trajectories circulate around the center of one scroll; the motion is rather predictable. At the brighter zones, however, the circulation becomes unstable and the trajectories tend to jump onto the other scroll. Due to this instability the predictability decreases.

In order to investigate the statistics of forecasting errors we take points from the second part of the time series and predict their successors. The forecasting interval T lasts 10 delay units corresponding to 1 ms. Then the predicted successors are compared with those really recorded and the error is calculated. In this context we denote by errors the difference vector between the predicted and the observed state in the reconstructed state space at the end of each forecasting time interval T. Figure 4 shows the statistical distribution of the errors occuring in 16 055 forecasts (solid bars). The distribution is dominated by moderate errors, but large and very large errors do occur rather frequently, too.

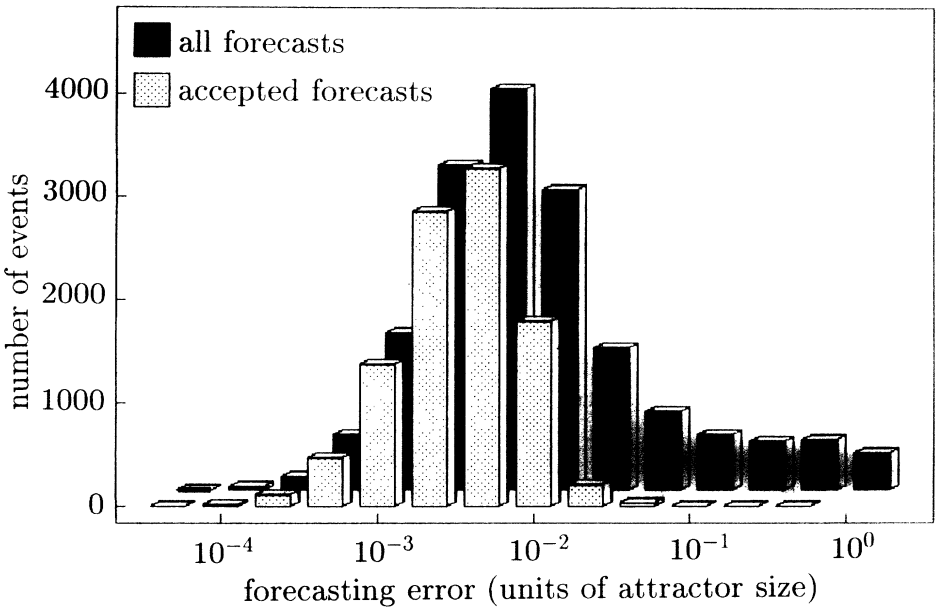

FIG. 4. Logarithmic plot of the distribution of relative forecast errors. The solid bars display the frequency of errors that occur if all forecasts are accepted. If forecasts with low predictability ($\lambda_{\text{eff}}^{(1)} > 100\ \text{s}^{-1}$) are rejected the distribution shown as hatched bars is obtained. Obviously the occurrence of large errors is reduced remarkably.

A second processor of the parallel computer system also calculates forecasts in the same way as the one described above, but it simultaneously calculates the corresponding effective Lyapunov exponents. According to their value all forecasts with an effective Lyapunov exponent above 100 s^{-1} are rejected. In Fig. 4 the resulting error statistics is shown by hatched bars. The number of accepted forecasts is 10 140, i.e., 63% of the total number of forecasts. Here the distribution of the smaller errors looks about the same as in the experiment above. The right part of the diagram, however, reveals a drastic reduction of the frequency of large errors. Nearly all the remaining forecast errors are smaller than or of the order of 1% compared to the size of the attractor. We quantify the feasibility of our method by calculation of the ratio of the average forecasting errors with and without consideration of the predictability. The average forecasting error of the accepted forecasts is 92% less than the one of all forecasts.

The effect, of course, depends strongly on the choice of the admitted effective Lyapunov exponent. For a larger border, less forecasts are rejected and, of course, the mean error is not reduced as much as for smaller borders. If, for example, we admit all forecasts for which $\lambda_{\text{eff}}^{(1)}$ in the initial state is $\lambda_{\text{eff}}^{(1)} \leq 200\ \text{s}^{-1}$ we achieve an error reduction of 86%, rejecting 18% of the forecasts. In a practical situation one might choose the border in a way that the number of forecasts and the average error are in good compromise.

We have chosen the parameter setting of Chua's circuit well in the regime, where the double scroll attractor exists. If we vary the resistor R, for example, the average time that the system stays on the same scroll is changed. For smaller R this time decreases, for larger ones it becomes longer. Since the jumps from one scroll to the other one are the less predictable phases of motion, the size of the zones of decreased predictability on the attractor changes. This leads to only slightly varying values of the ratio of average forecasting errors with and without consideration of predictability, when R is changed.

One might ask how much time passes until forecasts are accepted again if the system has just developed to a state with low predictability. In order to answer this question we plot in Fig. 5 a piece of a time series measured at the setup. Every point on the trajectory is marked where a forecast is calculated. When a forecast is rejected we plot a square, otherwise we plot a cross. The range of admitted Lyapunov exponents is $\lambda_{\text{eff}}^{(1)} \leq 200\ \text{s}^{-1}$. Additionally we display the length of the forecasting interval T. From the figure it becomes clear that forecasts are mainly rejected in a time interval of the length of about T before a jump from one scroll to the other. Nevertheless in our example the accepted forecasts are rather dense so that intervals where no forecasts are at hand are shorter than T.

In conclusion the mean error in forecasts of chaotic motions can be reduced drastically by consideration of the variance of predictability for different initial conditions. No ex-

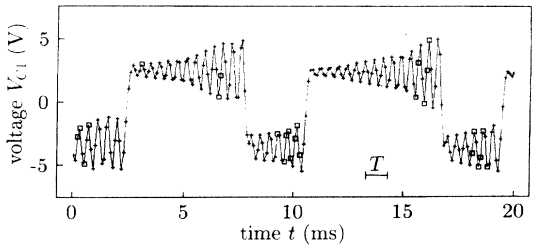

FIG. 5. The solid line displays a segment of a time series measured at the experimental setup. We mark all points where forecasts for the time interval T have been calculated. If $\lambda_{\text{eff}}^{(1)} \leq 200\ \text{s}^{-1}$, a cross is plotted, otherwise a square is plotted.

plicit model of the dynamics of the system is needed to calculate forecasts as well as predictabilities. Useful applications of the method are given, if one can wait to forecast the motion of the system, until the system is in a state with high predictability. As an example not really realistic yet, imagine a situation when the profit of some investments is strongly related to the reliability of forecasts made for the chaotic motion of a certain economical variable. The method we propose is to invest founding on an encouraging forecast only when the simultaneously calculated predictability is large enough.

More detailed investigations and applications of our method to other test systems are planned to be published elsewhere [19].

We would like to thank U. Linketscher, S. Berndt, and H. Heng for stimulating discussions. The electronic setup was built by U. Linketscher. This work was supported by the Deutsche Forschungsgemeinschaft via the "Sonderforschungsbereich 185, Nichtlineare Dynamik."

[1] J.-P. Eckmann and D. Ruelle, Rev. Mod. Phys. **57**, 617 (1985).
[2] P. Grassberger, R. Badii, and A. Politi, J. Stat. Phys. **51**, 135 (1988).
[3] H. D. I. Abarbanel, R. Brown, and M. B. Kennel, Int. J. Mod. Phys. B **5**, 1347 (1991).
[4] H. D. I. Abarbanel, R. Brown, and M. B. Kennel, J. Nonlinear Sci. **1**, 175 (1991).
[5] R. Doerner, B. Hübinger, W. Martienssen, S. Großmann, and S. Thomae, Chaos Solitons Fractals **1**, 553 (1991).
[6] R. Doerner, B. Hübinger, W. Martienssen, S. Großmann, and S. Thomae (unpublished).
[7] P. Cvitanović, Phys. Rev. Lett. **61**, 2729 (1988).
[8] D. Auerbach, B. O'Shaughnessy, and I. Procaccia, Phys. Rev. A **37**, 2234 (1988).
[9] B. Eckhardt, in *Quantum Chaos*, Lecture Notes for the International School of Physics "Enrico Fermi," Varenna, 1991, edited by G. Casati, I. Guarneri, and U. Smilansky (North-Holland, Amsterdam, 1993), pp. 77–111.
[10] F. Takens, in *Dynamical Systems and Turbulence, Warwick, 1980*, edited by D. A. Rand and L.-S. Young (Springer, Berlin, 1981), p. 366.
[11] J.-P. Eckmann, S. O. Kamphorst, D. Ruelle, and S. Ciliberto, Phys. Rev. A **34**, 4971 (1986).
[12] R. Brown, P. Bryant, and H. D. I. Abarbanel, Phys. Rev. A **43**, 2787 (1991).
[13] M. P. Kennedy, Frequenz **46**, 66 (1992).
[14] T. Matsumoto, IEEE Trans. Circuits Syst. **CAS-31**, 1055 (1984).
[15] *Chua's Circuit: A Paradigm for Chaos*, edited by R. N. Madan (World Scientific, Singapore, 1993).
[16] M. Komuro, R. Tokunaga, T. Matsumoto, L. O. Chua, and A. Hotta, Int. J. Bifurc. and Chaos **1**, 139 (1991), and references therein.
[17] P. Grassberger and I. Procaccia, Phys. Rev. Lett. **50**, 346 (1983).
[18] H. D. I. Abarbanel, R. Brown, and J. B. Kadtke, Phys. Rev. A **41**, 1782 (1990).
[19] R. Doerner, B. Hübinger, U. Linketscher, and W. Martienssen (unpublished).

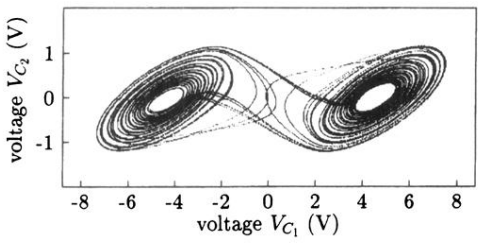

FIG. 2. The double-scroll attractor of Chua's circuit projected onto the (V_{C1}, V_{C2}) plane.

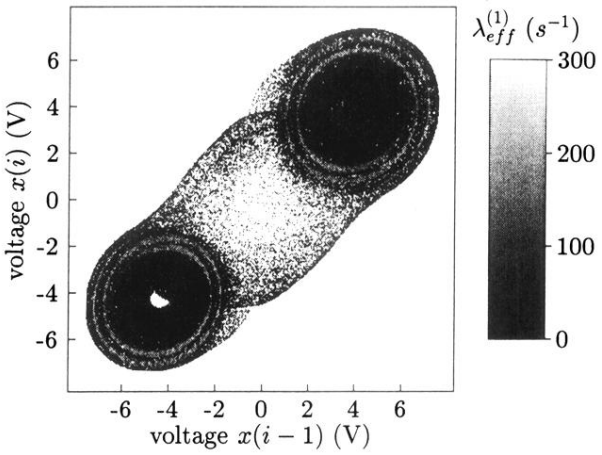

FIG. 3. A predictability portrait of the reconstructed double-scroll attractor. The forecasting interval is $T = 1$ ms. Note the spiral structure on each of the two scrolls. Between the scrolls the brightness is caused by the low density of points, not by a large effective Lyapunov exponent.

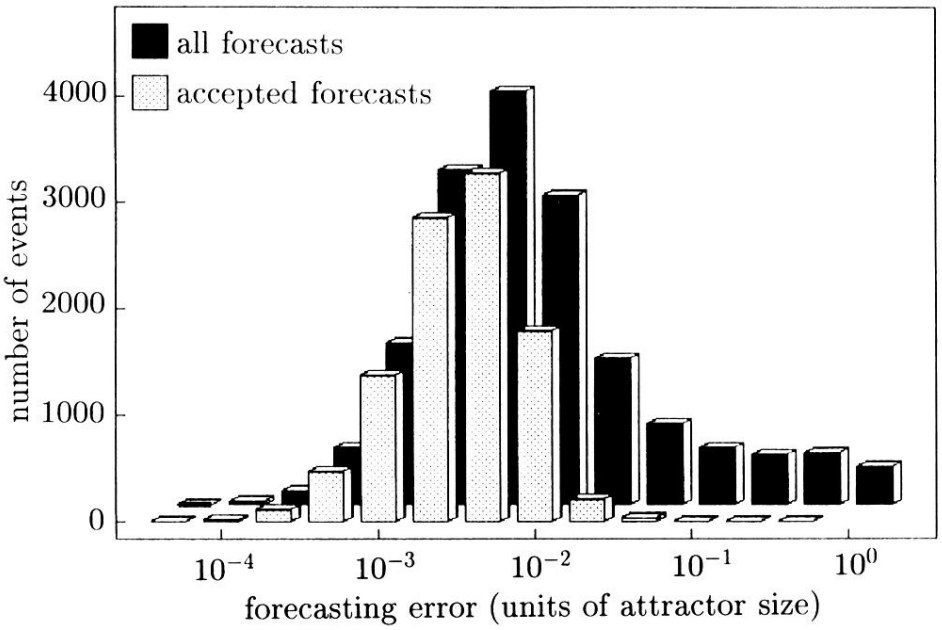

FIG. 4. Logarithmic plot of the distribution of relative forecast errors. The solid bars display the frequency of errors that occur if all forecasts are accepted. If forecasts with low predictability ($\lambda_{\text{eff}}^{(1)} > 100\ \text{s}^{-1}$) are rejected the distribution shown as hatched bars is obtained. Obviously the occurrence of large errors is reduced remarkably.